Published in final edited form as:
*Cell*. 2012 August 31; 150(5): 1055–1067. doi:10.1016/j.cell.2012.06.052.

# Role of Leaky Neuronal Ryanodine Receptors in Stress-Induced Cognitive Dysfunction

**Xiaoping Liu**[1], **Matthew J. Betzenhauser**[1], **Steve Reiken**[1], **Albano C. Meli**[1], **Wenjun Xie**[1], **Bi-Xing Chen**[1], **Ottavio Arancio**[2], and **Andrew R. Marks**[1,*]

[1]Clyde and Helen Wu Center for Molecular Cardiology, Department of Physiology and Cellular Biophysics, Columbia University College of Physicians and Surgeons

[2]Taub Institute for Research on Alzheimer's Disease and the Aging Brain, Department of Pathology and Cell Biology, Columbia University College of Physicians and Surgeons, New York, NY 10032, USA

## Summary

The type 2 ryanodine receptor/calcium release channel (RyR2), required for excitation-contraction coupling in the heart, is abundant in the brain. Chronic stress induces catecholamine biosynthesis and release, stimulating β-adrenergic receptors and activating cAMP signaling pathways in neurons. In a murine chronic restraint stress model neuronal RyR2 were phosphorylated by protein kinase A (PKA), oxidized and nitrosylated, resulting in depletion of the stabilizing subunit calstabin2 (FKBP12.6) from the channel complex and intracellular calcium leak. Stress-induced cognitive dysfunction, including deficits in learning and memory, and reduced long-term potentiation (LTP) at the hippocampal CA3-CA1 connection, were rescued by oral administration of S107, a novel compound developed in our laboratory that stabilizes RyR2-calstabin2 interaction, or by genetic ablation of the RyR2 PKA phosphorylation site at serine 2808. Thus, neuronal RyR2 remodeling contributes to stress-induced cognitive dysfunction. Leaky RyR2 could be a therapeutic target for treatment of stress-induced cognitive dysfunction.

## Introduction

Acute stress enhances cognitive function via activation of the sympathetic nervous system as part of the “fight-or-flight” response (McEwen and Sapolsky, 1995). In contrast, chronic stress causes cognitive dysfunction associated with glucocorticoid-induced hippocampal neuron damage (McEwen and Sapolsky, 1995). However, the precise mechanisms underlying stress-induced cognitive dysfunction remain poorly understood and there is currently no effective therapy.

Intracellular calcium ($Ca^{2+}$) homeostasis plays a crucial role in neuron survival and function. Neuronal $Ca^{2+}$ influx is mediated through voltage-gated channels and/or receptor-



*Correspondence: Andrew R. Marks, M.D., Columbia University College of Physicians and Surgeons, Department of Physiology and Cellular Biophysics, Russ Berrie Medical Sciences Pavilion, Room 520, 1150 St. Nicholas Ave., New York, NY 10032, USA, Phone (212) 851-5340; Fax (212) 851-5345, arm42@columbia.edu.

**Competing Financial Interests:** Dr. Andrew R. Marks is a consultant for a start-up company, ARMGO Pharma Inc., which is targeting RyR channels for therapeutic purposes.

operated channels activated by neurotransmitters. Intracellular $Ca^{2+}$ release occurs via ryanodine receptors (RyRs) and inositol (1,4,5)-trisphosphate receptors (IP3Rs) on the endoplasmic reticulum (ER) (Berridge et al., 2003). There are three isoforms of RyR in the brain. RyR1 and RyR2 are both expressed in the hippocampus. RyR2 expression is up-regulated in rat hippocampus following intensive training tasks (Cavallaro et al., 1997; Zhao et al., 2000). RyR2 knock-down impairs performance of mice in passive avoidance tests (Galeotti et al., 2008) whereas RyR1 knock-down did not (Galeotti et al., 2008).

$Ca^{2+}$ released into the cytoplasm is pumped back into the ER by the ER Ca-ATPase (SERCA) or removed from the cell by the plasma membrane Ca-ATPase (PMCA) and $Na^{+}$/$Ca^{2+}$ exchanger. Altered $Ca^{2+}$ homeostasis contributes to neuronal degeneration and cell death (Mattson, 2007) and defective postsynaptic signaling, presynaptic control of neurotransmitter release, and long-term synaptic plasticity (Berridge, 1998; Fitzjohn and Collingridge, 2002).

We have shown that binding of the subunit calstabin2 (FKBP12.6) to RyR2 channels in the heart is impaired under stress conditions by PKA phosphorylation at Serine 2808 (Wehrens et al., 2005) and oxidation/nitrosylation of the channel such that calstabin2 depleted RyR2 channels leak intracellular $Ca^{2+}$ (Shan et al., 2010a; Shan et al., 2010b). A novel class of drugs (derivatives of 1,4-benzothiazepines) known as intracellular calcium release channel stabilizers, or Rycals, (e.g. S107 and JTV-519) (Bellinger et al., 2008b), prevent stress-induced depletion of calstabin from RyR and fix the pathological intracellular $Ca^{2+}$ leak. Rycals inhibit heart failure progression in mice (Shan et al., 2010a), and prevent catecholamine-induced arrhythmias (Lehnart et al., 2008; Shan et al., 2010a; Wehrens et al., 2004; Yano et al., 2003).

We now show that stress-induced oxidation, nitrosylation and PKA hyperphosphorylation deplete calstabin2 from brain RyR2 resulting in leaky channels that contribute to stress-induced cognitive dysfunction in mice. The orally available small molecule S107 decreased ER $Ca^{2+}$ leak via neuronal RyR2 and prevented stress-induced cognitive dysfunction. Genetic ablation of the RyR2 PKA phosphorylation site in RyR2-S2808A$^{+/+}$ mice (Shan et al., 2010b; Wehrens et al., 2005) also protects against stress-induced cognitive dysfunction. Taken together, these results establish a crucial role for leaky neuronal RyR2 in stress-induced cognitive dysfunction and suggest a potential therapeutic approach to preventing stress-induced cognitive dysfunction and post-traumatic stress disorder (PTSD).

## Results

### Hippocampal Stress Response

WT and RyR2-S2808A$^{+/+}$ mice were subjected to chronic restraint stress (Copeland et al., 2005; Fukui et al., 1997; Patel et al., 2004) with or without treatment with the Rycal S107 in the drinking water (Figure. 1A). There was a >2-fold sustained increase in plasma corticosterone (CORT) in WT and RyR-S2808A$^{+/+}$ mice following 3 weeks of chronic restraint stress (Aguilera, 1994; Carrasco and Van de Kar, 2003; McEwen, 2004, 2007) (Figure 1B, S1C). The immediate early gene c-Fos was significantly elevated after acute stress, and to a lesser degree after acute stress following chronic stress indicating some blunting of the HPA axis (Figure S1D-F) consistent with previous reports (Perrotti et al., 2004). The transcription factors CREB and ERK regulate tyrosine hydroxylase and catecholamine biosynthesis, and are phosphorylated under stress conditions (Brazelton et al., 2000; Impey et al., 1998; Liu et al., 2005; Liu et al., 2008; Sabban et al., 2004; Shaywitz and Greenberg, 1999). There was a significant increase in CREB (pCREB) and ERK (pERK) phosphorylation in hippocampal, cortical, and whole brain from stressed mice, consistent

with a general stress response in the brain (Figure 1C-E, S2) and increased PKA activity (Figure S2G). PKA catalytic or regulatory subunits were unchanged (Figure 1E).

CRF, ACTH and CORT were significantly increased at 15 min after termination of chronic stress in all stressed groups (Figure S1A-C). CRF and ACTH fell to control levels one hr post-chronic stress (Figures S1A, B), however CORT levels remained significantly elevated at 24 hrs post-stress indicating a persistent stress response (Figure S1C). There was a significant but blunted elevation of CRF, ACTH and CORT after acute stress in chronically stressed WT and RyR2-S2808A$^{+/+}$ mice (Figure S1A-C), indicating that the HPA-axis was intact but blunted (Figure S1A-C).

## Stress-induced Remodeling of the RyR2 Macromolecular Complex

Neuronal RyR2 were PKA hyperphosphorylated, oxidized, *S*-nitrosylated and depleted of calstabin2 in hippocampal and whole brain (Figures 2A-E, S3A-E). Neuronal ER SERCA activity was unchanged in stressed mice (Figure S3F). S107 given in drinking water (75 mg/kg/d) prior to and during the stress protocol prevented calstabin2 depletion from the RyR2 macromolecular complex without altering PKA phosphorylation, oxidation or *S*-nitrosylation of RyR2 (Figure 2E). S107 improves cardiac and skeletal muscle function (Andersson et al., 2011; Bellinger et al., 2009; Shan et al., 2010a; Shan et al., 2010b). To show that the effects of S107 in the present study were due to its neural as opposed to extraneural actions, mice were treated with a related Rycal (S36, 75 mg/Kg/day) that also improves cardiac and skeletal muscle function but does not cross the blood-brain-barrier. In contrast to S107, S36 did not prevent calstabin2 depletion from neuronal RyR2 in hippocampal samples from stressed mice (Figure S4A-E).

PKA, $H_2O_2$ and Noc-12 individually caused a ~2-fold decrease in the binding affinity of calstabin2 to RyR2 ($p<0.05$) (Figures 2F-H, S5A,B), and in combination a ~ 4-fold decrease in the binding affinity of calstabin2 to RyR2 ($p<0.01$) (Figures 2H, S5A,B) as determined by $^{35}$S-calstabin2 binding, and ~80% depletion of calstabin2 from RyR2 assessed by co-immunoprecipitation ($p<0.01$) (Figure 2F,G). Anti-calstabin2 antibody co-immunoprecipitated RyR2 (Figure S5C). There was no stress-induced change in total neuronal RyR2 or calstabin2 (Figure S5D).

PKA phosphorylation, oxidation and nitrosylation of RyR2 cause calstabin2 depletion from cardiac RyR2 during heart failure (Lehnart et al., 2004; Shan et al., 2010a; Wehrens et al., 2004). Mice harboring RyR2 channels that cannot be phosphorylated by PKA (RyR2-S2808A$^{+/+}$) are protected against heart failure progression (Shan et al., 2010b; Wehrens et al., 2006). Stress-induced depletion of calstabin2 from hippocampal or whole brain RyR2 was not observed in RyR2-S2808A$^{+/+}$ mice (Figures 2A-E, S3A-E). Thus, S107 or genetic ablation of the RyR2 PKA phosphorylation site prevent calstabin2 depletion from neuronal RyR2 in stressed mice.

## Leaky neuronal RyR2 Channels in Chronically Stressed Mice *Single-channel Activity*

The stress-induced remodeling of the cardiac RyR2 macromolecular complex results in "leaky" channels (Lehnart et al., 2008; Shan et al., 2010a; Wehrens et al., 2004). We sought to determine whether stress-induced remodeling of hippocampal RyR2 channels also results in leaky channels with higher single-channel open probabilities (Po) under resting conditions (e.g. with low cytosolic activating [$Ca^{2+}$]). In WT control mice the RyR Po was essentially zero at low cytosolic [$Ca^{2+}$] (150 nM) (Figure 3A and F), whereas RyR channels from stressed mice exhibited a significantly increased Po (Figure 3B and F). RyR channels from S107 treated stressed mice exhibited low Po, similar to non-stressed mice (Figure 3C and F). RyR in non-stressed and stressed RyR2-S2808A+/+ mice showed no increased Po (Figure

3D-F). Whole brain RyR exhibited similar increases in single-channel Po and normalization when mice were treated with S107 compared to hippocampal RyR channels (Figure S3H).

**Intracellular $Ca^{2+}$ Leak—**Stress significantly increased ER $Ca^{2+}$ leak (33.13 ± 4.2% of uptake in stress, n=7, versus 21.75 ± 1.82 % of uptake in non-stress, n=9, $p<0.05$ by one-way ANOVA) (Figure 3G, H). Treatment with S107 in the drinking water prior to and during the stress significantly reduced ER $Ca^{2+}$ leak (13.51 ± 1.72% of uptake in S107 treated stress, n=7, versus stress, $p<0.05$ by one-way ANOVA) (Figure 3G and H). There was no significant difference in ER $Ca^{2+}$ leak between stressed (10.10 ± 0.67 % of uptake, n=7) and non-stressed RyR2-S2808A$^{+/+}$ (10.14 ± 1.74 % of uptake, n=7, $p>0.05$ by one-way ANOVA) or between WT and RyR2-S2808A$^{+/+}$ mice (Figure 3G and H).

Thus, chronic stress-induced remodeling of neuronal RyR2 channels caused increased single-channel Po under resting conditions and ER $Ca^{2+}$ leak that was prevented by treatment with S107 or genetic ablation of the RyR2-S2808 PKA phosphorylation site.

## Impaired Cognitive Function and Hippocampal Synaptic Plasticity in Stressed Mice

Mice were examined using a Morris Water Maze (MWM) to assess hippocampal-dependent learning and memory (Morris, 1984). Three month-old WT non-stressed and stressed mice exhibited no differences in swimming velocities indicating that there was no locomotor defect (Figure S3G). The time spent to reach the hidden platform (escape latency) was prolonged in WT-stressed mice (50.85 ± 3.09s, n=21) compared to non-stressed control mice (28.39 ± 3.79s, n=21, $p<0.05$) at day 3 of the 5-day trial (Figure 4A). Stressed WT mice exhibited prolonged escape latency on days 3-5, $p<0.01$, indicating impaired learning due to chronic restraint stress (Figure 4A).

S107 in the drinking water (75 mg/kg/day) significantly reduced escape latency at day 3 (26.61 ± 3.31s, n=22) compared to the non-treated stressed mice (50.85 ± 3.09s, n=21, $p<0.05$) (Figure 4A). A probe trial was performed on day 6 in which the mice attempted to locate the previously hidden platform that had been removed. The percentage of time spent in the target quadrant and the number of target crossings in control non-stressed WT mice (52.3 ± 4.8%; 4.3 ± 0.59, n=21) were significantly higher than those in stressed WT mice (32.50±2.86%, n=21, $p<0.05$; 1.59 ± 0.36, n=21, $p<0.05$) (Figure 4B and C), suggesting impaired learning in stressed mice. The stress-induced learning impairment was prevented by S107 treatment as both the time spent in the target quadrant and the number of target crossings were increased in the treated animals (54.58 ± 2.56%, n=22, $p<0.05$; 5.67 ± 0.34, n=22, $p<0.05$) (Figure 4B and C). A lower dose of S107 (50 mg/kg/day), or beginning treatment after the chronic stress did not prevent stress-induced cognitive dysfunction as assessed using the MWM (Figure S4I-K). The rycal S36 (75 mg/kg/day), which does not cross the BBB, did not improve either the time spent in the target quadrant or the number of target crossings (Figure S4F-H).

The novel object recognition (NOR) task was used to assess hippocampal-type memory (Bevins and Besheer, 2006; Denny et al., 2011). There were no significant differences in the total exploration duration among groups in phase-1, the habituation phase, when mice were exposed to two-identical objects (Figure S6). In phase-2, the testing phase, when one object was replaced by a novel object, WT stressed mice failed to discriminate between the novel object and the constant object. The discrimination index (DI) of WT stressed mice (49.22 ± 2.16, n=11) was significantly lower than controls (82.44 ± 1.50, n=12, $p<0.05$) (Figure S6). S107 treatment improved the DI of stressed mice to control level (82.59 ± 2.24, n=9, $p<0.05$ compared to stressed WT) (Figure S6). In agreement with the MWM results, the NOR test demonstrated that chronic stress impairs memory in WT mice, and pharmacologic (S107) rescues this impairment.

Elevated plus maze (EPM) (Pellow et al., 1985) and open-field (Hall, 1934) tests were used to assess anxiety and spontaneous activity in stressed WT mice. In the EPM, mice were placed at the center of the plus maze and allowed to move freely for 5 m. The time-spent in the closed-arm and open-arm, the total number of entries to the closed-arm and open-arm were recorded. WT stressed mice spent significantly longer time in the closed-arm (236.57 ± 9.18s, n=21) than non-stressed controls (197.86 ± 5.51s, n=21, $p<0.05$ by two-way ANOVA), and spent significantly shorter time in the open-arm (11.14 ± 3.24s, n=21) than controls (44.21 ± 5.0s, n=21, $p<0.05$ by two-way ANOVA) (Figure S7). The ratio of time-spent in the open-arm versus closed-arm was significantly reduced in WT stressed mice (0.06 ± 0.03, n=21) compared to non-stressed controls (0.22 ± 0.05, n=21, $p<0.05$ by two-way ANOVA) (Figure 4D). There were no significant differences in total number of entries to the closed-arm among experimental groups, but there were significantly fewer entries to the open-arm in WT stressed mice (1.43 ± 0.4, n=21) than controls (4.79 ± 0.46, n=21, $p<0.05$ by two-way ANOVA) (Figure S7). The ratio of the number of open-arm entries vs closed-arm entries was significantly reduced in WT stressed mice (0.23 ± 0.08, n=21) compared to non-stressed controls (0.47 ± 0.08, n=21, $p<0.05$ by two-way ANOVA) (Figure 4E). S107 treatment significantly reduced total time-spent in the closed-arm (180.94 ± 4.57s, n=22, $p<0.05$ by two-way ANOVA), but improved total time-spent in the open-arm (53.44 ± 4.79s, n=22, $p<0.05$ by two-way ANOVA) in WT stressed mice (Figure S7). S107 treatment also significantly improved the ratios of time-spent on the open-arm versus closed-arm and the number of open-arm entries versus closed-arm entries in stressed mice (0.29 ± 0.07, n=22, $p<0.001$; 0.48 ± 0.06, n=22, $p<0.001$ by two-way ANOVA) (Figure 4E). There were no differences in these two ratios when S107 treated non-stressed mice were compared to non-treated controls (0.27 ± 0.05, n=14, $p=0.194$; 0.51 ± 0.07, n=14, $p=0.24$ by two-way ANOVA) (Figure 4D and E) suggesting that the positive effects of S107 are not manifested in the absence of stress.

In the open-field test, mice were placed at the center of the experimental chamber and allowed to move for 6 m. The number of visits to the center area and peripheral area were recorded and analyzed. Within the first 3 m and the second 3 m, the ratios of the number of center visits versus peripheral visits for WT stressed mice were significantly lower (0.08 ± 0.02; 0.09 ± 0.03, n=22) than those of non-stressed WT controls (0.14 ± 0.03, n=21, $p<0.01$; 0.32 ± 0.06, $p<0.01$ by one-way ANOVA) (Figure 4F). These results are consistent with reduced spontaneous exploratory activity in the stressed mice. S107 significantly improved the exploratory activity and behavioral response to a novel environment in stressed mice as demonstrated by the increased ratios of the number of center visits versus periphery visits within both the first 3 m and second 3 m (0.20 ± 0.04, $p<0.05$; 0.22 ± 0.02, n=22, $p<0.01$ by one-way ANOVA) (Figure 4F). Taken together, the behavioral studies demonstrate that stressed mice have cognitive dysfunction manifested as impaired learning and memory, increased anxiety and reduced spontaneous exploratory activity. Pharmacologic (S107) therapy targeting the RyR channel prevented stress-induced cognitive dysfunction suggesting that neuronal ER $Ca^{2+}$ leak causes cognitive dysfunction during stress.

Post-synaptic plasticity of hippocampal neurons was assessed using electrophysiological recordings of long-term potentiation (LTP) which reflects long-term hippocampal-type memory. Theta-burst stimulation (TBS) was used (12 bursts at 5 Hz, each consisting of four pulses delivered at 100 Hz) (Patterson et al., 2001) at the CA3-CA1 connection in hippocampal slices. LTP was reduced in stressed WT mice (205.9 ± 13.2%, n=7) compared to non-stressed mice (354.1 ± 26.1%, n=7, $p<0.001$ by two-way ANOVA) (Figure 4G). Treatment with S107 in the drinking water during stress prevented LTP reduction (330.4 ± 17.6%, n=7, $p<0.001$) (Figure 4G). The input-output curve was not altered by either stress or S107 treatment (Figure 4H). Thus, the stress-induced impairment of hippocampal post-synaptic plasticity was significantly improved by S107.

### Improved Synaptic and Cognitive Function in Stressed RyR2-S2808A$^{+/+}$ mice

RyR2-S2808A$^{+/+}$ mice that harbor RyR2 that cannot be PKA phosphorylated were subjected to behavioral testing after 3-weeks of chronic restraint stress. In MWM tests RyR2-S2808A$^{+/+}$ mice showed the same escape latency (18.62 ± 3.05s, n=13) as WT mice (19.16 ± 3.0s, n=15, p=0.87 by one-way ANOVA) (Figure 5A) indicating normal cognitive function in the RyR2-S2808A$^{+/+}$ mice. The time spent in the target quadrant and the number of target crossings also showed no differences between RyR2-S2808A$^{+/+}$ (49.82 ± 4.87%; 3.73 ± 0.45 crossings, n=13) and WT mice (54.4 ± 3.62%, n=15, $p$=0.23; 4.13 ± 0.39 crossings, n=15, $p$=0.25) (Figure 5B and C). Stress failed to alter the escape latency in RyR2-S2808A$^{+/+}$ mice, at day 5 of the training trial there were no significant differences in escape latency (17.43 ± 1.40s, n=16) compared to non-stressed RyR2-S2808A$^{+/+}$ mice (18.62 ± 3.05s, n=13, $p$=0.85 by one-way ANOVA) (Figure 4A). Probe trials similarly showed no deficits in stressed RyR2-S2808A$^{+/+}$ mice which exhibited the same time spent in the target quadrant and number of target crossings (50.44 ± 2.78%; 4.33 ± 0.31 crossings, n=16) as non-stressed RyR2-S2808A$^{+/+}$ (49.82 ± 4.87%, n=13, $p$=0.40; 3.73 ± 0.45, n=13, $p$=0.14) (Figure 5B and C). There were no differences in swimming velocity between groups in the MWM tests (Figure S3G).

The NOR test indicated there was no effect of stress on memory in the RyR2-S2808A$^{+/+}$ mice as the DI in phase-2 was unchanged (Figure S6).

EPM testing showed no significant differences in total time-spent in the closed-arm and open-arm between stressed RyR2-S2808A$^{+/+}$ (161.31 ± 3.43 s in closed-arm, 44.77 ± 7.55 s in open-arm, n=16) and non-stressed RyR2-S2808A$^{+/+}$ mice (166.21 ± 7.25 s in closed-arm, n=15, $p$=0.38; 47.64 ± 6.46 s in open-arm, n=15, $p$=0.65 by two-way ANOVA) (Figure S7). There were no significant differences in total number of entries to the closed-arm and open-arm between stressed RyR2-S2808A$^{+/+}$ (9.15 ± 1.23 to the closed-arm, 4.62 ± 0.77 to the open-arm, n=16) and non-stressed RyR2-S2808A$^{+/+}$ mice (9.43 ± 1.19 to the closed-arm, n=15, $p$=0.80; 4.86 ± 0.72 to the open-arm, n=15, $p$=0.95 by two-way ANOVA) (Figure S7). There were no differences in time-spent in the open-arm versus closed-arm between stressed RyR2-S2808A$^{+/+}$ (0.29 ± 0.34, n=16) and non-stressed RyR2-S2808A$^{+/+}$ (0.29 ± 0.31, n=15, $p$=0.92 by two-way ANOVA) (Figure 5D). There were also no differences in the number of open-arm entries versus closed-arm between stressed RyR2-S2808A$^{+/+}$ (0.56 ± 0.06, n=16) and non-stressed RyR2-S2808A$^{+/+}$ (0.59 ± 0.10, n=15, $p$=0.79 by two-way ANOVA) (Figure 5E), suggesting no significant changes in the level of anxiety in RyR2-S2808A$^{+/+}$ mice under stress.

Open-field tests revealed that within the first 3 m and the second 3 m stress failed to alter the ratios of the number of center visits versus peripheral visits in RyR2-S2808A$^{+/+}$ mice (0.17 ± 0.01, n=16 in stressed; 0.15 ± 0.02, n=15 in non-stressed, $p$=0.22 by one-way ANOVA) (Figure 5F), indicating no significant stress-induced changes in spontaneous activity in the RyR2-S2808A$^{+/+}$ mice.

Electrophysiological recordings revealed no differences in LTP between the RyR2-S2808A$^{+/+}$ (325.4 ± 11.6%, n=7) and WT mice (329.4 ± 18.5%, n=7, $p$=0.88 assessed by two-way ANOVA) (Figure 5G). Chronic stress failed to affect LTP in the RyR2-S2808A$^{+/+}$ mice (313.9 ± 17.1%, n=7, $p$=0.56, assessed by 2-way ANOVA) (Figure 5G). Two-way ANOVA revealed no differences in the input-output curves between WT and RyR2-S2808A$^{+/+}$ mice (Figure 5H), and there were no differences in the input-output relationships between stressed and non-stressed RyR2-S2808A$^{+/+}$ mice (Figure 5H).

Thus, stress-induced defects in cognitive function and post-synaptic plasticity in hippocampal neurons were ameliorated by preserving RyR2-calstabin2 interaction either by administering S107 or by genetic ablation of the RyR2 PKA phosphorylation site.

## RyR1 Does Not Play a Major Role in Chronic Stress-induced Cognitive Dysfunction

In addition to RyR2, RyR1, which is required for skeletal muscle excitation-contraction coupling, is expressed in specific regions of the brain, including the hippocampus and cerebellum (Giannini et al., 1995). We have demonstrated a role for PKA hyperphosphorylation at Serine 2844 and oxidation and nitrosylation of RyR1 in promoting SR $Ca^{2+}$ leak in skeletal muscle during extreme exercise, muscular dystrophy and aging (Andersson et al., 2011; Bellinger et al., 2008a; Bellinger et al., 2009; Bellinger et al., 2008b). PKA hyperphosphorylation at Serine 2844 and nitrosylation and oxidation of RyR1 cause depletion of calstabin1 from the channel complex destabilizing the closed state at low cytosolic activating [$Ca^{2+}$] (~150 nM) (Marx et al., 2000; Reiken et al., 2003b; Ward et al., 2003).

We subjected RyR1-S2844A$^{+/+}$ knock-in mice, which harbor RyR1 channels that cannot be PKA phosphorylated, to the stress protocol described in Figure 1A. Elevated plasma corticosterone levels (Figure 6A) and hippocampal pCREB and pERK phosphorylation confirmed the extent of stress in the RyR1-S2844A$^{+/+}$ mice (Figure 6B-D).

Neuronal RyR1 were PKA hyperphosphorylated in hippocampus (Figure 6E and I) and whole brain (Figure S3H-K) following stress, and *S*-nitrosylated and oxidized (Figure 6E, G, and H). There was minimal depletion of calstabin1 from RyR1 (Figure 6E and I) in hippocampus compared to a significant reduction of calstabin1 from RyR1 in the whole brain (Figure S5E-G). Treatment with S107 prevented calstabin1 depletion from the RyR1 macromolecular complex in the whole brain (Figure S5E-G).

WT mice and RyR1-S2844A$^{+/+}$ knock-in mice were examined using MWM, EPM, and open-field tasks. In the MWM task, ablation of the PKA phosphorylation site of RyR1 at Serine 2844 did not prevent learning impairment in stressed RyR1-S2844A$^{+/+}$ mice characterized by prolonged escape latency after day 3 (47.3 ± 1.9s, n=12, $p$<0.05) compared to the non-stressed mice (37.5±2.8s, n=30) (Figure 7A) and less time spent in target quadrant (22.2 ± 0.2%, n=12, $p$<0.05) and reduced target crossings (1.3 ± 0.1, n=12, $p$<0.05) on the day 6 probe trial (Figure 7B and C). There were also no differences between RyR1-S2844A$^{+/+}$ and WT in the escape latency observed during the 5 day trial ($p$=0.95 by one-way ANOVA) (Figure 7A). The time spent in the target quadrant and the number of target crossings were not significantly different between WT (45.3 ± 2.3%; 3.8 ± 0.4, n=30) and non-stressed RyR1-S2844A$^{+/+}$ mice (44.3 ± 2.7%, n=30, $p$=0.38; 3.1 ± 0.5, n=30, $p$=0.15) (Figure 7B and C). No differences in swimming velocity among the groups were observed (Figure S3G).

EPM tests showed no significant differences in time-spent in the open-arm versus the closed-arm between RyR1-S2844A$^{+/+}$ (0.29 ± 0.04, n=30) and WT mice (0.26 ± 0.04, n=30, $p$=0.66 by two-way ANOVA) (Figure 7D). There were also no differences in the number of open-arm versus closed-arm entries between RyR1-S2844A$^{+/+}$ (0.47 ± 0.07, n=30) and WT (0.40 ± 0.07, n=30, $p$=0.55 by two-way ANOVA) (Figure 7D). Ablation of the RyR1 PKA phosphorylation site at serine 2844 failed to prevent the increase in anxiety in the stressed RyR1-S2844A$^{+/+}$ mice. The time-spent on the open-arm versus closed-arm and the number of entries to the open-arm versus closed-arm in stressed RyR1-S2844A$^{+/+}$ mice were significantly reduced (0.08 ± 0.02, n=12, $p$<0.05; 0.29 ± 0.05, n=12, $p$<0.05 by two-way ANOVA) compared to the non-stressed RyR1-S2844A$^{+/+}$ mice (Figure 7E). Open-field tests from same group of animals as in the MWM and EPM revealed that, within the first 3 m and

the second 3 m, the ratios of the number of center visits versus peripheral visits in stressed RyR1-S2844A$^{+/+}$ mice were significantly lower (0.11 ± 0.02; 0.12 ± 0.02, n=12) than those of non-stressed RyR1-S2844A$^{+/+}$ (0.17 ± 0.02, n= 30, $p<0.05$; 0.32 ± 0.03, $p<0.05$ by one-way ANOVA) (Figure 7F). There were no differences between the RyR1-S2844A$^{+/+}$ and WT mice in the open-field tests ($p=0.46$, $p=0.79$ by one-way ANOVA) (Figure 7F). Thus, unlike RyR2, remodeling of the RyR1 macromolecular complex does not appear to play a role in stress-induced cognitive dysfunction.

## Discussion

There is a well established link between impaired learning, working and long-term memory and somatic factors, including mental stress and chronic diseases (Etgen et al., 2009). Stress affects the function and morphology of neurons (Kim and Diamond, 2002), and hippocampal neurogenesis (Mirescu and Gould, 2006). Moreover, it has been proposed that these effects could underlie neuropsychiatric disorders and PTSD (Airan et al., 2007; Mirescu and Gould, 2006). Long-term, chronic stress is a major contributor to the development of neuropsychiatric, cardiovascular, and autoimmune diseases, cancer and propensity to self-administer drugs of abuse (McEwen, 2008). The stress response is characterized by a rapid increase in norepinephrine (NE) and epinephrine (Epi) to maintain systemic “homeostasis” (Cannon, 1929; McMahon et al., 1992; Tsuda and Tanaka, 1985; Zigmond et al., 1989). Increased sympathetic activation and urinary NE and/or Epi concentrations are consistently observed in patients with PTSD (Southwick et al., 1999; Yehuda et al., 1998) suggesting long-term chronic stress (Miller and McEwen, 2006; Sherin and Nemeroff, 2011). Despite all of these parallels between chronic stress and PTSD, one potential caveat is that the chronic restraint stress model used in the present study likely does not recapitulate all of the parameters of PTSD.

Current therapy for PTSD remains largely supportive, and not mechanism based. Here we examined the potential role of stress-induced intracellular $Ca^{2+}$ leak due to stress-induced remodeling of RyR/calcium release channels that have not previously been implicated in stress-induced cognitive dysfunction. PKA phosphorylation of RyR1 and RyR2 (Marx et al., 2000; Reiken et al., 2003a; Reiken et al., 2003b) at serine 2844 or 2808, respectively increases channel activity and intracellular $Ca^{2+}$ release during acute stress (e.g. exercise) (Marx et al., 2000; Reiken et al., 2003b). RyR dysfunction and pathologic intracellular $Ca^{2+}$ leak occur during intense chronic β-adrenergic stimulation due to sympathetic hyperactivity (Marx et al., 2000). We have developed a novel RyR-targeted small molecule Rycal (S107) that stabilizes the RyR1 and RyR2 closed states of PKA hyperphosphorylated, and oxidized/nitrosylated channels and prevents intracellular $Ca^{2+}$ leak induced pathophysiology in relevant animal models of heart failure, exercise-induced arrhythmias, muscular dystrophies and sarcopenia (Andersson et al., 2011; Bellinger et al., 2009; Bellinger et al., 2008b; Lehnart et al., 2006; Wehrens et al., 2005; Wehrens et al., 2004).

Elevated intracellular $Ca^{2+}$ has been associated with cognitive dysfunction due to brain injury (Deshpande et al., 2008), and neuro-degeneration including Alzheimer's and aging (Berridge, 2010; Keefe et al., 1989; Khachaturian, 1994). One of the downstream consequences of increased RyR2-mediated $Ca^{2+}$ leak could be abnormal action potential conduction in hippocampal pyramidal neurons (Svoboda et al., 1997). Neuronal cell death could also be a consequence of $Ca^{2+}$ leak since sustained increases in cytosolic $Ca^{2+}$ resulting from excessive glutamate mediate excitotoxic cell death (Choi, 1988a, b; Hartley et al., 1993). Other downstream targets include $Ca^{2+}$-dependent proteases and transcriptional activation through CaMKII, PKA and MAPK mediated activation of immediate early genes (Ghosh and Greenberg, 1995).

Intracellular $Ca^{2+}$ homeostasis is also regulated by the IP3Rs and SERCA pumps on the ER (Berridge et al., 2003). Studies have shown improved cognitive function in mice due to blockade of IP3R in prefrontal cortex under stress condition (Brennan et al., 2008). Another study showed increased IP3R-mediated ER $Ca^{2+}$ release in hippocampal neurons during hypoxia (Bickler et al., 2009). We did not observe stress-induced effects on IP3R1 (Figure S5H) or SERCA (Figure S3F) in contrast to the stress-induced remodeling of RyR2 that rendered the channels leaky. Although RyR1 and RyR2 are structurally and functionally homologous the fact that RyR1-S2844A$^{+/+}$ mice did not protect against stress-induced cognitive dysfunction whereas RyR2-S2808A$^{+/+}$ did suggests that RyR2 but RyR1 is involved in stressed-induced cognitive dysfunction.

Thus, neuronal RyR2 remodeling by PKA hyperphosphorylation, oxidation and nitrosylation plays an important role in chronic stress-induced cognitive dysfunction. Furthermore, leaky neuronal RyR2 channels could be a potential pharmacological target to ameliorate chronic stress-induced cognitive dysfunction and PTSD.

## Experimental Procedures

### Animals and Restraint Stress Protocol

Wild type (WT) C57BL/6 mice and age-matched RyR2-S2808A$^{+/+}$ and RyR1-S2844A$^{+/+}$ knock-in mice (Wehrens et al., 2005) were subjected to restraint stress in 50 ml plastic restraint tubes (Plas-Labs Broome-Style Rodent Restrainer, from Fisher Scientific), without food and water from 6PM to 9AM for 3 weeks (Copeland et al., 2005). Schedules for applying restraint stress and performing cognition function tests are illustrated in Figure 1A. Investigators were blinded with respect to genotype and treatment.

### Statistical Analysis

MWM and open-field tests were analyzed using one-way ANOVA and comparison *t*-test. EPM and LTP measurement were analyzed using two-way ANOVA and comparison *t*-test. All other data were expressed as mean ± SEM. The results of $Ca^{2+}$ leak assay were analyzed by one-way ANOVA with Bonferroni correction. Minimum statistically significant differences were established at $P < 0.05$.

## Supplementary Material

Refer to Web version on PubMed Central for supplementary material.

## Acknowledgments

The authors thank Drs. Steven Siegelbaum and Michael Shelanski for helpful comments and Shi-Xian Deng for synthesis of S107. This work was supported by RO1-HL56180 and RO1-NS049442.

## References

Aguilera G. Regulation of pituitary ACTH secretion during chronic stress. Front Neuroendocrinol. 1994; 15:321–350. [PubMed: 7895891]

Airan RD, Meltzer LA, Roy M, Gong Y, Chen H, Deisseroth K. High-speed imaging reveals neurophysiological links to behavior in an animal model of depression. Science. 2007; 317:819–823. [PubMed: 17615305]

Andersson DC, Betzenhauser MJ, Reiken S, Meli AC, Umanskaya A, Xie W, Shiomi T, Zalk R, Lacampagne A, Marks AR. Ryanodine receptor oxidation causes intracellular calcium leak and muscle weakness in aging. Cell Metab. 2011; 14:196–207. [PubMed: 21803290]

Bellinger AM, Mongillo M, Marks AR. Stressed out: the skeletal muscle ryanodine receptor as a target of stress. J Clin Invest. 2008a; 118:445–453. [PubMed: 18246195]

Bellinger AM, Reiken S, Carlson C, Mongillo M, Liu X, Rothman L, Matecki S, Lacampagne A, Marks AR. Hypernitrosylated ryanodine receptor calcium release channels are leaky in dystrophic muscle. Nat Med. 2009; 15:325–330. [PubMed: 19198614]

Bellinger AM, Reiken S, Dura M, Murphy PW, Deng SX, Landry DW, Nieman D, Lehnart SE, Samaru M, LaCampagne A, et al. Remodeling of ryanodine receptor complex causes “leaky” channels: a molecular mechanism for decreased exercise capacity. Proc Natl Acad Sci U S A. 2008b; 105:2198–2202. [PubMed: 18268335]

Berridge MJ. Neuronal calcium signaling. Neuron. 1998; 21:13–26. [PubMed: 9697848]

Berridge MJ. Calcium hypothesis of Alzheimer's disease. Pflugers Arch. 2010; 459:441–449. [PubMed: 19795132]

Berridge MJ, Bootman MD, Roderick HL. Calcium signalling: dynamics, homeostasis and remodelling. Nat Rev Mol Cell Biol. 2003; 4:517–529. [PubMed: 12838335]

Bevins RA, Besheer J. Object recognition in rats and mice: a one-trial non-matching-to-sample learning task to study ‘recognition memory’. Nat Protoc. 2006; 1:1306–1311. [PubMed: 17406415]

Bickler PE, Fahlman CS, Gray J, McKleroy W. Inositol 1,4,5-triphosphate receptors and NAD(P)H mediate Ca2+ signaling required for hypoxic preconditioning of hippocampal neurons. Neuroscience. 2009; 160:51–60. [PubMed: 19217932]

Brazelton TR, Rossi FM, Keshet GI, Blau HM. From marrow to brain: expression of neuronal phenotypes in adult mice. Science. 2000; 290:1775–1779. [PubMed: 11099418]

Brennan AR, Dolinsky B, Vu MA, Stanley M, Yeckel MF, Arnsten AF. Blockade of IP3-mediated SK channel signaling in the rat medial prefrontal cortex improves spatial working memory. Learn Mem. 2008; 15:93–96. [PubMed: 18285467]

Cannon W. Organization for physiological homeostasis. Physiol Rev. 1929; 9:399–431.

Carrasco GA, Van de Kar LD. Neuroendocrine pharmacology of stress. Eur J Pharmacol. 2003; 463:235–272. [PubMed: 12600714]

Cavallaro S, Meiri N, Yi CL, Musco S, Ma W, Goldberg J, Alkon DL. Late memory-related genes in the hippocampus revealed by RNA fingerprinting. Proc Natl Acad Sci U S A. 1997; 94:9669–9673. [PubMed: 9275181]

Choi DW. Calcium-mediated neurotoxicity: relationship to specific channel types and role in ischemic damage. Trends Neurosci. 1988a; 11:465–469. [PubMed: 2469166]

Choi DW. Glutamate neurotoxicity and diseases of the nervous system. Neuron. 1988b; 1:623–634. [PubMed: 2908446]

Copeland BJ, Neff NH, Hadjiconstantinou M. Enhanced dopamine uptake in the striatum following repeated restraint stress. Synapse. 2005; 57:167–174. [PubMed: 15945060]

Denny CA, Burghardt NS, Schachter DM, Hen R, Drew MR. 4- to 6-week-old adult-born hippocampal neurons influence novelty-evoked exploration and contextual fear conditioning. Hippocampus. 2011

Deshpande LS, Sun DA, Sombati S, Baranova A, Wilson MS, Attkisson E, Hamm RJ, DeLorenzo RJ. Alterations in neuronal calcium levels are associated with cognitive deficits after traumatic brain injury. Neurosci Lett. 2008; 441:115–119. [PubMed: 18583041]

Etgen T, Bronner M, Sander D, Bickel H, Sander K, Forstl H. [Somatic factors in cognitive impairment]. Fortschr Neurol Psychiatr. 2009; 77:72–82. [PubMed: 19221969]

Fitzjohn SM, Collingridge GL. Calcium stores and synaptic plasticity. Cell Calcium. 2002; 32:405–411. [PubMed: 12543099]

Fukui Y, Sudo N, Yu XN, Nukina H, Sogawa H, Kubo C. The restraint stress-induced reduction in lymphocyte cell number in lymphoid organs correlates with the suppression of in vivo antibody production. J Neuroimmunol. 1997; 79:211–217. [PubMed: 9394794]

Galeotti N, Quattrone A, Vivoli E, Norcini M, Bartolini A, Ghelardini C. Different involvement of type 1, 2, and 3 ryanodine receptors in memory processes. Learn Mem. 2008; 15:315–323. [PubMed: 18441289]

Ghosh A, Greenberg ME. Calcium signaling in neurons: molecular mechanisms and cellular consequences. Science. 1995; 268:239–247. [PubMed: 7716515]

Giannini G, Conti A, Mammarella S, Scrobogna M, Sorrentino V. The ryanodine receptor/calcium channel genes are widely and differentially expressed in murine brain and peripheral tissues. J Cell Biol. 1995; 128:893–904. [PubMed: 7876312]

Hall CS. Emotional behavior in the rat: Defecation and urination as measures of individual edifferences in emotionality. J Comp Psychol. 1934; 18:385–403.

Hartley DM, Kurth MC, Bjerkness L, Weiss JH, Choi DW. Glutamate receptor-induced 45Ca2+ accumulation in cortical cell culture correlates with subsequent neuronal degeneration. J Neurosci. 1993; 13:1993–2000. [PubMed: 7683048]

Impey S, Obrietan K, Wong ST, Poser S, Yano S, Wayman G, Deloulme JC, Chan G, Storm DR. Cross talk between ERK and PKA is required for Ca2+ stimulation of CREB-dependent transcription and ERK nuclear translocation. Neuron. 1998; 21:869–883. [PubMed: 9808472]

Keefe KA, Salamone JD, Zigmond MJ, Stricker EM. Paradoxical kinesia in parkinsonism is not caused by dopamine release. Studies in an animal model. Arch Neurol. 1989; 46:1070–1075. [PubMed: 2508609]

Khachaturian ZS. Calcium hypothesis of Alzheimer's disease and brain aging. Ann N Y Acad Sci. 1994; 747:1–11. [PubMed: 7847664]

Kim JJ, Diamond DM. The stressed hippocampus, synaptic plasticity and lost memories. Nat Rev Neurosci. 2002; 3:453–462. [PubMed: 12042880]

Lehnart SE, Mongillo M, Bellinger A, Lindegger N, Chen BX, Hsueh W, Reiken S, Wronska A, Drew LJ, Ward CW, et al. Leaky Ca2+ release channel/ryanodine receptor 2 causes seizures and sudden cardiac death in mice. J Clin Invest. 2008; 118:2230–2245. [PubMed: 18483626]

Lehnart SE, Terrenoire C, Reiken S, Wehrens XH, Song LS, Tillman EJ, Mancarella S, Coromilas J, Lederer WJ, Kass RS, et al. Stabilization of cardiac ryanodine receptor prevents intracellular calcium leak and arrhythmias. Proc Natl Acad Sci U S A. 2006; 103:7906–7910. [PubMed: 16672364]

Lehnart SE, Wehrens XH, Kushnir A, Marks AR. Cardiac ryanodine receptor function and regulation in heart disease. Ann N Y Acad Sci. 2004; 1015:144–159. [PubMed: 15201156]

Liu X, Kvetnansky R, Serova L, Sollas A, Sabban EL. Increased susceptibility to transcriptional changes with novel stressor in adrenal medulla of rats exposed to prolonged cold stress. Brain Res Mol Brain Res. 2005; 141:19–29. [PubMed: 16169632]

Liu X, Serova L, Kvetnansky R, Sabban EL. Identifying the stress transcriptome in the adrenal medulla following acute and repeated immobilization. Ann N Y Acad Sci. 2008; 1148:1–28. [PubMed: 19120088]

Marx SO, Reiken S, Hisamatsu Y, Jayaraman T, Burkhoff D, Rosemblit N, Marks AR. PKA phosphorylation dissociates FKBP12.6 from the calcium release channel (ryanodine receptor): defective regulation in failing hearts. Cell. 2000; 101:365–376. [PubMed: 10830164]

Mattson MP. Calcium and neurodegeneration. Aging Cell. 2007; 6:337–350. [PubMed: 17328689]

McEwen BS. Protection and damage from acute and chronic stress: allostasis and allostatic overload and relevance to the pathophysiology of psychiatric disorders. Ann N Y Acad Sci. 2004; 1032:1–7. [PubMed: 15677391]

McEwen BS. Physiology and neurobiology of stress and adaptation: central role of the brain. Physiol Rev. 2007; 87:873–904. [PubMed: 17615391]

McEwen BS. Central effects of stress hormones in health and disease: Understanding the protective and damaging effects of stress and stress mediators. Eur J Pharmacol. 2008; 583:174–185. [PubMed: 18282566]

McEwen BS, Sapolsky RM. Stress and cognitive function. Curr Opin Neurobiol. 1995; 5:205–216. [PubMed: 7620309]

McMahon A, Kvetnansky R, Fukuhara K, Weise VK, Kopin IJ, Sabban EL. Regulation of tyrosine hydroxylase and dopamine beta-hydroxylase mRNA levels in rat adrenals by a single and repeated immobilization stress. J Neurochem. 1992; 58:2124–2130. [PubMed: 1349344]

Miller MM, McEwen BS. Establishing an agenda for translational research on PTSD. Ann N Y Acad Sci. 2006; 1071:294–312. [PubMed: 16891579]

Mirescu C, Gould E. Stress and adult neurogenesis. Hippocampus. 2006; 16:233–238. [PubMed: 16411244]

Morris R. Developments of a water-maze procedure for studying spatial learning in the rat. J Neurosci Methods. 1984; 11:47–60. [PubMed: 6471907]

Patel S, Roelke CT, Rademacher DJ, Cullinan WE, Hillard CJ. Endocannabinoid signaling negatively modulates stress-induced activation of the hypothalamic-pituitary-adrenal axis. Endocrinology. 2004; 145:5431–5438. [PubMed: 15331569]

Patterson SL, Pittenger C, Morozov A, Martin KC, Scanlin H, Drake C, Kandel ER. Some forms of cAMP-mediated long-lasting potentiation are associated with release of BDNF and nuclear translocation of phospho-MAP kinase. Neuron. 2001; 32:123–140. [PubMed: 11604144]

Pellow S, Chopin P, File SE, Briley M. Validation of open:closed arm entries in an elevated plus-maze as a measure of anxiety in the rat. J Neurosci Methods. 1985; 14:149–167. [PubMed: 2864480]

Perrotti LI, Hadeishi Y, Ulery PG, Barrot M, Monteggia L, Duman RS, Nestler EJ. Induction of deltaFosB in reward-related brain structures after chronic stress. J Neurosci. 2004; 24:10594–10602. [PubMed: 15564575]

Reiken S, Gaburjakova M, Guatimosim S, Gomez AM, D'Armiento J, Burkhoff D, Wang J, Vassort G, Lederer WJ, Marks AR. Protein kinase A phosphorylation of the cardiac calcium release channel (ryanodine receptor) in normal and failing hearts. Role of phosphatases and response to isoproterenol. J Biol Chem. 2003a; 278:444–453. [PubMed: 12401811]

Reiken S, Lacampagne A, Zhou H, Kherani A, Lehnart SE, Ward C, Huang F, Gaburjakova M, Gaburjakova J, Rosemblit N, et al. PKA phosphorylation activates the calcium release channel (ryanodine receptor) in skeletal muscle: defective regulation in heart failure. J Cell Biol. 2003b; 160:919–928. [PubMed: 12629052]

Sabban EL, Hebert MA, Liu X, Nankova B, Serova L. Differential effects of stress on gene transcription factors in catecholaminergic systems. Ann N Y Acad Sci. 2004; 1032:130–140. [PubMed: 15677400]

Shan J, Betzenhauser MJ, Kushnir A, Reiken S, Meli AC, Wronska A, Dura M, Chen BX, Marks AR. Role of chronic ryanodine receptor phosphorylation in heart failure and beta-adrenergic receptor blockade in mice. J Clin Invest. 2010a; 120:4375–4387. [PubMed: 21099115]

Shan J, Kushnir A, Betzenhauser MJ, Reiken S, Li J, Lehnart SE, Lindegger N, Mongillo M, Mohler PJ, Marks AR. Phosphorylation of the ryanodine receptor mediates the cardiac fight or flight response in mice. J Clin Invest. 2010b; 120:4388–4398. [PubMed: 21099118]

Shaywitz AJ, Greenberg ME. CREB: a stimulus-induced transcription factor activated by a diverse array of extracellular signals. Annu Rev Biochem. 1999; 68:821–861. [PubMed: 10872467]

Sherin JE, Nemeroff CB. Post-traumatic stress disorder: the neurobiological impact of psychological trauma. Dialogues Clin Neurosci. 2011; 13:263–278. [PubMed: 22034143]

Southwick SM, Bremner JD, Rasmusson A, Morgan CA 3rd, Arnsten A, Charney DS. Role of norepinephrine in the pathophysiology and treatment of posttraumatic stress disorder. Biol Psychiatry. 1999; 46:1192–1204. [PubMed: 10560025]

Svoboda K, Denk W, Kleinfeld D, Tank DW. In vivo dendritic calcium dynamics in neocortical pyramidal neurons. Nature. 1997; 385:161–165. [PubMed: 8990119]

Tsuda A, Tanaka M. Differential changes in noradrenaline turnover in specific regions of rat brain produced by controllable and uncontrollable shocks. Behav Neurosci. 1985; 99:802–817. [PubMed: 3843302]

Ward CW, Reiken S, Marks AR, Marty I, Vassort G, Lacampagne A. Defects in ryanodine receptor calcium release in skeletal muscle from post-myocardial infarct rats. FASEB J. 2003; 17:1517–1519. [PubMed: 12824280]

Wehrens XH, Lehnart SE, Reiken S, van der Nagel R, Morales R, Sun J, Cheng Z, Deng SX, de Windt LJ, Landry DW, et al. Enhancing calstabin binding to ryanodine receptors improves cardiac and skeletal muscle function in heart failure. Proc Natl Acad Sci U S A. 2005; 102:9607–9612. [PubMed: 15972811]

Wehrens XH, Lehnart SE, Reiken S, Vest JA, Wronska A, Marks AR. Ryanodine receptor/calcium release channel PKA phosphorylation: a critical mediator of heart failure progression. Proc Natl Acad Sci U S A. 2006; 103:511–518. [PubMed: 16407108]

Wehrens XH, Lehnart SE, Reiken SR, Deng SX, Vest JA, Cervantes D, Coromilas J, Landry DW, Marks AR. Protection from cardiac arrhythmia through ryanodine receptor-stabilizing protein calstabin2. Science. 2004; 304:292–296. [PubMed: 15073377]

Yano M, Kobayashi S, Kohno M, Doi M, Tokuhisa T, Okuda S, Suetsugu M, Hisaoka T, Obayashi M, Ohkusa T, et al. FKBP12.6-mediated stabilization of calcium-release channel (ryanodine receptor) as a novel therapeutic strategy against heart failure. Circulation. 2003; 107:477–484. [PubMed: 12551874]

Yehuda R, Schmeidler J, Giller EL Jr, Siever LJ, Binder-Brynes K. Relationship between posttraumatic stress disorder characteristics of Holocaust survivors and their adult offspring. Am J Psychiatry. 1998; 155:841–843. [PubMed: 9619162]

Zhao W, Meiri N, Xu H, Cavallaro S, Quattrone A, Zhang L, Alkon DL. Spatial learning induced changes in expression of the ryanodine type II receptor in the rat hippocampus. FASEB J. 2000; 14:290–300. [PubMed: 10657985]

Zigmond RE, Schwarzschild MA, Rittenhouse AR. Acute regulation of tyrosine hydroxylase by nerve activity and by neurotransmitters via phosphorylation. Annu Rev Neurosci. 1989; 12:415–461. [PubMed: 2564757]

## Highlights

- Leaky hippocampal RyR2 channels contribute to stress-induced cognitive dysfunction
- RyR2 PKA hyperphosphorylation & calstabin2 depletion cause intracellular $Ca^{2+}$ leak
- Pharmacologic or genetic inhibition of $Ca^{2+}$ leak prevent the cognitive dysfunction

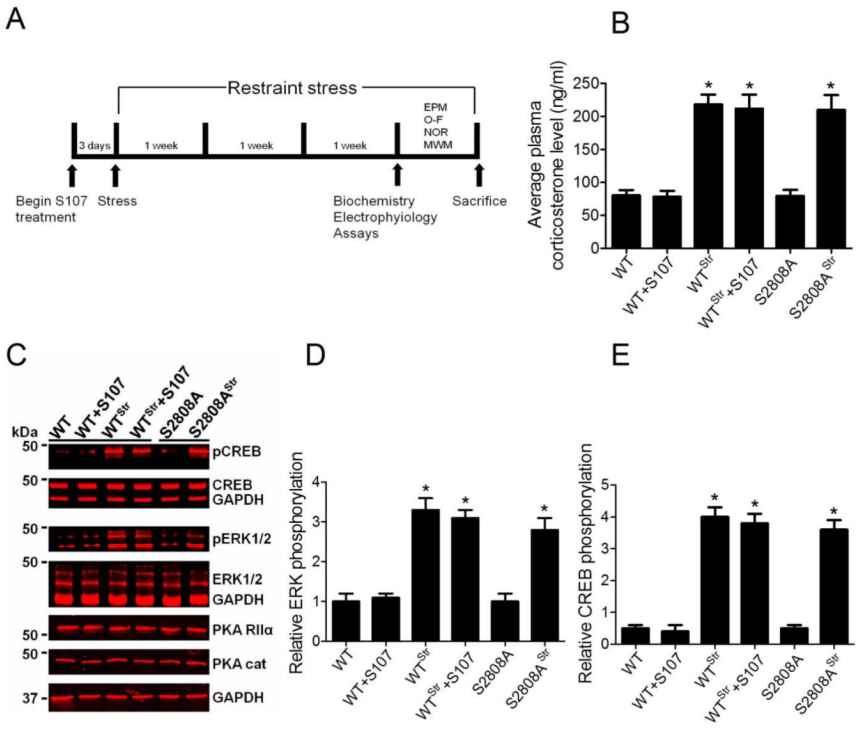


**Figure 1. Chronic Stress Response in WT and in the RyR2-S2808A$^{+/+}$Mice**

**(A)** Mice were randomly divided into groups as indicated. Stressed mice were subjected to chronic restraint stress in Plexiglas restraint tubes overnight daily for 3 weeks, S107 (75mg/Kg/day) in drinking water was begun 3 days before stress and throughout the experiment. **(B)** Plasma corticosterone levels were assayed in the morning. Data are mean ± S.E.M., n=4. **(C)** Representative immunoblots showing pCREB and pERK in control and stressed mice. Hippocampal samples were isolated immediately after 3-weeks of stress from WT and RyR2- S2808A$^{+/+}$ mice. **(D, E)** Summary data (mean ± S.E.M., n=5) are shown for pCREB **(C)** and pERK **(D)**. Total CREB, total ERK and GAPDH are loading controls. See also Figures S1.

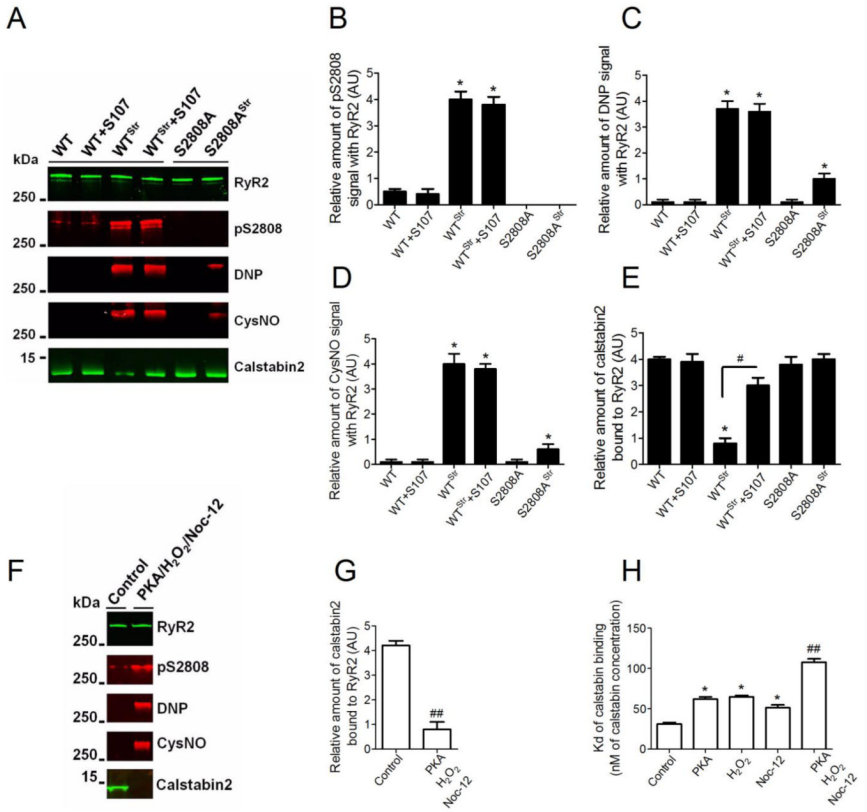


**Figure 2. Stress-induced Remodeling of Neuronal RyR2 Macromolecular Complexes**

**(A)** Hippocampal RyR2 was immunoprecipitated and immunoblotted to detect PKA hyperphosphorylation, oxidation and Cys *S*-nitrosylation of RyR2 and calstabin2 as previously described (Marx et al., 2000; Reiken et al., 2003b; Shan et al., 2010a; Shan et al., 2010b; Ward et al., 2003) **(B-E)** Summary data for RyR2-pS2808, Cys S-nitrosylation, DNP (oxidation), and calstabin2. Data are mean ± S.E.M., *, **, $^{\#}p<0.05$, n=5. The mean for the unstressed control was set = 1.0. **(F)** ER microsomes were resuspended and treated with PKA (40units), $H_2O_2$ (1mM), Noc-12 (100μM) separately, or in combination. Treated microsomes were immunoprecipitated and immunoblotted with the antibodies described in **A-E. (G)** Summary data for F, immunoblot data for calstabin2/RyR2. **(H)** Kds for $^{35}$S-calstabin2 binding to RyR2. Data are mean ± S.E.M., *, **, $^{\#}p<0.05$, $^{\#\#}p<0.01$, n=5. See also Figures S3-S5.

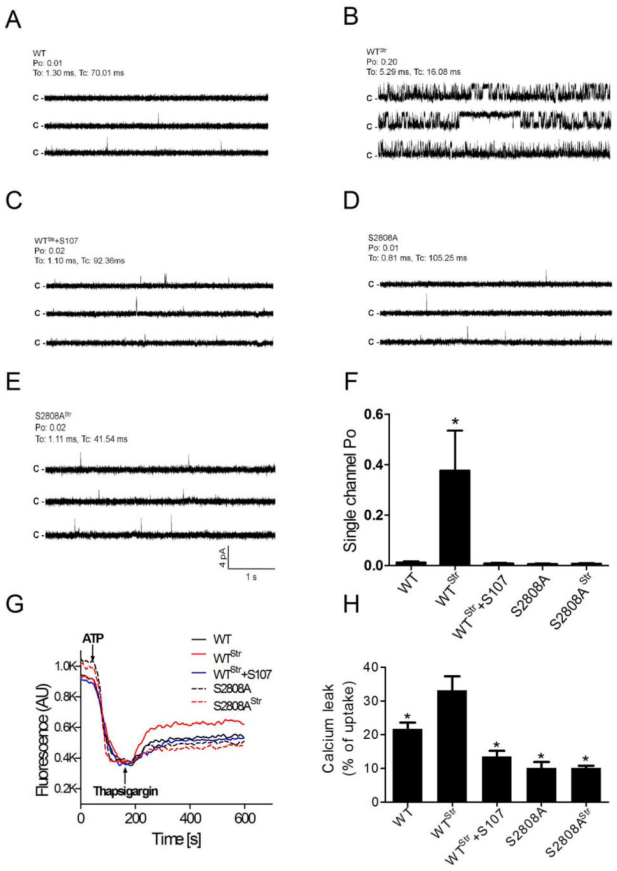


**Figure 3. Single Channel Recordings of Hippocampal RyR Channels from Stressed Mice**

**(A-C)** Representative hippocampal RyR single-channel current traces from control (WT, n=6) **(A)**, stress ($WT^{Str}$, n=5) **(B)**, S107 treated stress ($WT^{Str}$+S107, n=5) **(C),** RyR2-$S2808A^{+/+}$ (S2808A, n=4) **(D)**, and stressed RyR2-$S2808A^{+/+}$ mice ($S2808A^{Str}$, n=6) **(E)** examined with 150 nmol/L (nM) free cytosolic [$Ca^{2+}$] in the *cis* chamber. Channel openings are upward deflections and horizontal bars at the left of each trace indicate the closed (c-) state of the channels. For each group, channel activity is illustrated with 4 traces, each 5 s. RyR identity was confirmed by addition of 5 μmol/L (μM) ryanodine at the end of each experiment. The single channel open probability (Po), To (mean open time) and Tc (mean closed time) at 150 nmol/L free cytosolic [$Ca^{2+}$] are above the upper trace. **(F)** Summary of RyR2 single-channel Po with 150 nmol/L free cytosolic [$Ca^{2+}$] from RyR2-WT, RyR2-$WT^{Str}$, $WT^{Str}$+S107, S2808A and $S2808A^{Str}$. Data are mean ± S.E.M., *$p < 0.05$ vs. WT. **(G)** Representative traces of $Ca^{2+}$ leak from brain microsomes induced by addition of thapsigargin (3 μM). **(H)** $Ca^{2+}$ leak was calculated as the percentage of uptake. Data (mean ± S.E.M.) analysis was performed by one-way ANOVA, $p$=0.0001. Bonferroni post-test revealed *$p$<0.05 vs. $WT^{Str}$ (WT, n=9; $WT^{Str}$, n=7; $WT^{Str}$+S107, n=7; S2808A, n=4; S2808A+ST, n=4). See also Figure S3H-K.

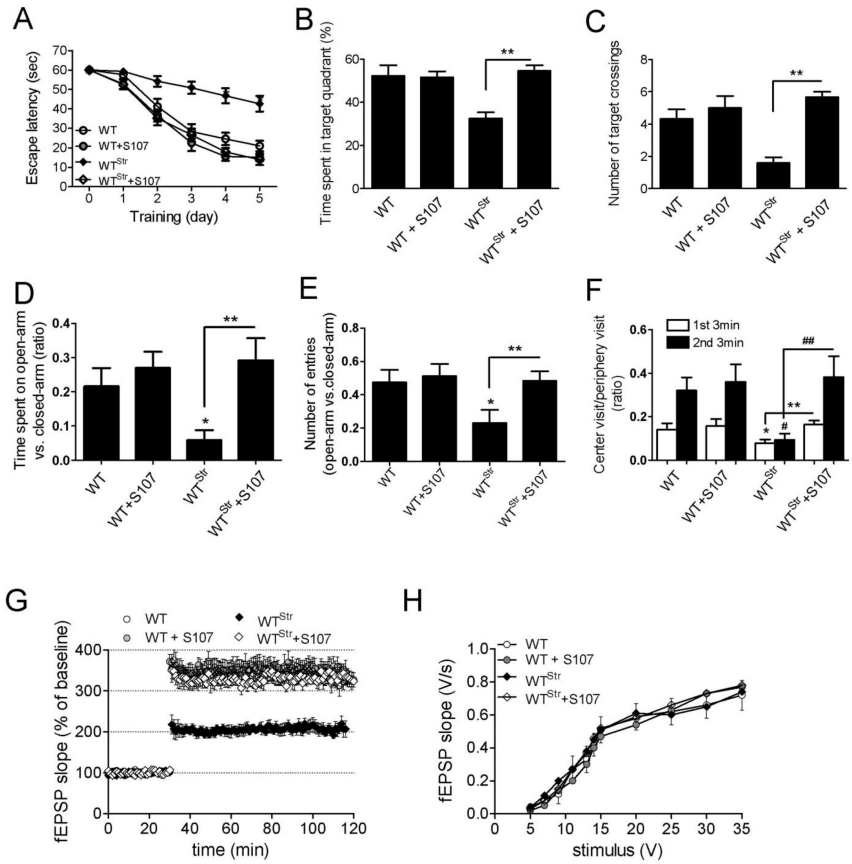


**Figure 4. Effects of Stress on Cognitive Function and Hippocampal Synaptic Plasticity**

**(A)** MWM escape latency for WT non-stressed control (WT, n=21), S107 treated WT non-stressed (WT+S107, n=14), WT stressed ($WT^{Str}$, n=21), and S107 treated stressed ($WT^{Str}$+S107, n=22). **(B, C)** Probe trials measuring time spent in the target quadrant and number of target crossings. <0.05. **(D, E)** EPM test on the same groups of mice. **(D)** Summary of ratios of time-spent on the open-arm versus closed-arm are shown. **(E)** Summary data of ratios of number of entries to the open-arm versus closed-arm are shown. **(F)** Open-field test from the same group of mice as shown in MWM and EPM tests. *$p$<0.05 versus non-stressed controls within the first 3 min, #$p$<0.05 versus non-stressed controls within the second 3 min. **(G)** Potentiation following theta-burst stimulation in the CA1 region of hippocampal slices from WT mice (WT, n=7), S107 treated control (WT+S107, n=7), stress ($WT^{Str}$, n=7), and S107 treated stress ($WT^{Str}$+S107, n=7). **(H)** Summary of field input-output relationships in the same slices as in **(G)**. All data are mean ± S.E.M. See also Figure S3G.

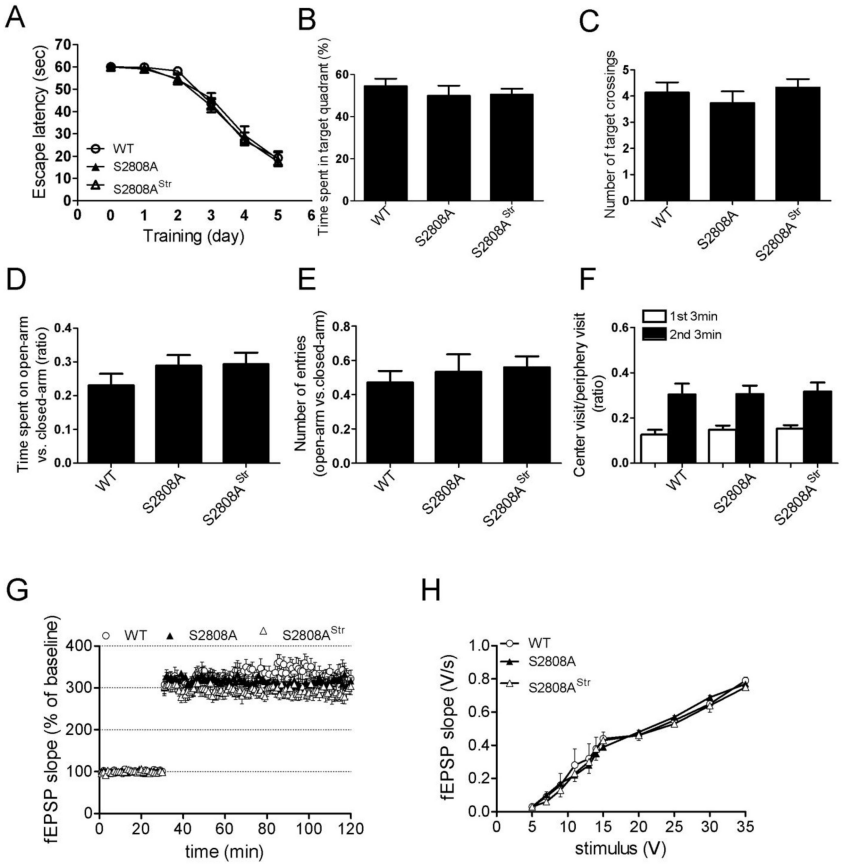


**Figure 5. Effects of Stress on Cognitive Function and Hippocampal Synaptic Plasticity in RyR2-S2808A$^{+/+}$Mice**

**(A)** MWM escape latency for WT (WT, n=15), RyR2-S2808A$^{+/+}$ non-stressed (S2808A, n=13), and RyR2-S2808A$^{+/+}$ stressed (S2808A$^{Str}$, n=16). **(B, C)** Probe trials after escape platform removed, *$p$<0.05. **(D, E)** EPM test in the same groups. **(D)** Summary data of ratios of time-spent on the open-arm versus closed-arm. **(E)** Summary data of ratios of number of entries to the open-arm versus closed-arm. **(F)** Open-field test from the same group of mice. Ratios of total time spent in the center area versus periphery area within first 3 min and 2nd 3 min. **(G)** Potentiation following theta-burst stimulation in the CA1 region of hippocampal slices from WT mice (WT, n=7), RyR2-S2808A$^{+/+}$ (S2808A, n=7) and stressed RyR2-S2808A$^{+/+}$ (S2808A$^{Str}$, n=7). **(H)** Field input-output relationships in the same slices as in **(G)**. See also Figures S3G-S7. All data are mean ± S.E.M.

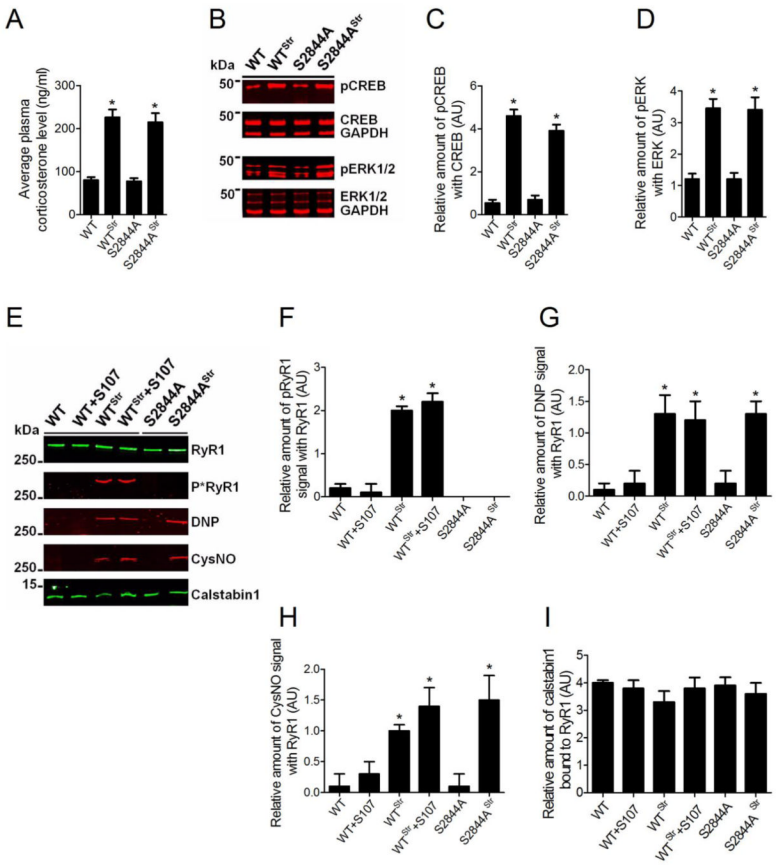


**Figure 6. Stress-induced Remodeling of RyR1 Complexes and Cognitive Function in RyR1-S2844A$^{+/+}$mice**

**(A)** RyR2-S2844A$^{+/+}$ mice were subjected to the restraint stress protocol in Figure 1A. Morning plasma corticosterone levels collected. n=4. **(B)** Representative immunoblots showing levels of hippocampal pCREB and pERK in control and stressed mice. Summary data for the levels of pCREB **(C)** and pERK **(D)**. Total CREB, total ERK and GAPDH were loading controls. **(E)** Representative immunoblots of RyR1 immunoprecipitated from whole brain samples from control (WT), WT stressed (WT$^{Str}$), RyR1-S2844A$^{+/+}$ (S2844A), and RyR1-S2844A$^{+/+}$ stressed (S2844A$^{Str}$) probed with antibodies showing PKA hyperphosphorylation, oxidation (DNP), Cys *S*-nitrosylation (CysNO) of RyR1, and co-immunoprecipitated calstabin1. **(F-I)** Summary data for phosphorylated RyR1, oxidized and nitrosylated RyR1, and calstabin1. *, **, $^{\#}p<0.05$, n=4. The mean for the unstressed WT control was taken as 1.0. All data are mean ± S.E.M. See also Figure S5E-G.

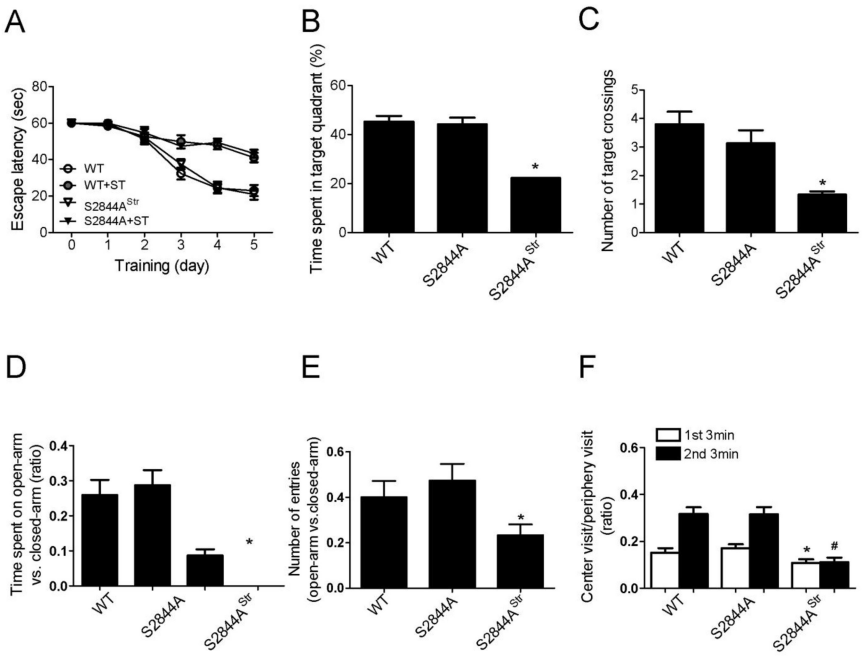


**Figure 7. Effects of Stress on Cognitive Function in RyR1-S2844A$^{+/+}$Mice**

**(A)** MWM escape latency in WT (WT, n=30), RyR1-S2844A$^{+/+}$ (S2844A, n=30), and stressed RyR1-S2844A$^{+/+}$ (S2844A$^{Str}$, n=12). **(B, C)** Probe trial after removal of escape platform, *$p$<0.05. **(D, E)** EPM in the same groups of mice. **(D)** Summary data for ratios of time-spent on the open-arm versus closed-arm are shown. **(E)** Summary data for ratios of number of entries to the open-arm versus closed-arm are shown. **(F)** Results of open-field test from the same groups of mice. Ratios of total time spent in the center area versus periphery area within first 3 min and 2nd 3 min are shown. All data are mean ± S.E.M. See also Figure S3G.